Dalton Transactions

Accepted Manuscript

This article can be cited before page numbers have been issued, to do this please use: D. Cao, T. Gao, Q. Fan and Z.T. Yu, *Dalton Trans.*, 2017, DOI: 10.1039/C7DT01337J.

This is an Accepted Manuscript, which has been through the Royal Society of Chemistry peer review process and has been accepted for publication.

Accepted Manuscripts are published online shortly after acceptance, before technical editing, formatting and proof reading. Using this free service, authors can make their results available to the community, in citable form, before we publish the edited article. We will replace this Accepted Manuscript with the edited and formatted Advance Article as soon as it is available.

You can find more information about Accepted Manuscripts in the author guidelines.

Please note that technical editing may introduce minor changes to the text and/or graphics, which may alter content. The journal's standard Terms & Conditions and the ethical guidelines, outlined in our author and reviewer resource centre, still apply. In no event shall the Royal Society of Chemistry be held responsible for any errors or omissions in this Accepted Manuscript or any consequences arising from the use of any information it contains.

ROYAL SOCIETY OF CHEMISTRY

rsc.li/dalton

View Article Online
DOI: 10.1039/C7DT01337J

Cyclometalated Ir(III) complexes based on 2-(2,4-difluorophenyl)-pyridine and 2,2'-(2-phenyl-1H-imidazole-4,5-diyl)dipyridine: acid/base-induced structural transformation and luminescence switching, and photocatalytic activity for hydrogen evolution†

Tai-Bao Gao,[a] Qianwenhao Fan,[a] Zhen-Tao Yu[b] and Deng-Ke Cao*[a]

Received (in XXX, XXX) Xth XXXXXXXXX 200X, Accepted Xth XXXXXXXXX 200X
First published on the web Xth XXXXXXXXX 200X
DOI: 10.1039/b000000x

Based on ligands dfppyH and pidpyH (Scheme 1), cyclometalated Ir(III) complexes $[Ir(dfppy)_2(pidpyH)](PF_6)$ **(1·PF$_6$)** and $[Ir(dfppy)_2(pidpy)]$ **(2)** have been synthesized. Crystal structures indicate that each $\{Ir(dfppy)_2\}^+$ unit is coordinated by a neutral ligand pidpyH in **1·PF$_6$**, while a $pidpy^-$ anion in **2**. The packing structure of **1·PF$_6$** only exhibits electrostatic interactions and van der Waals interactions among $[Ir(dfppy)_2(pidpyH)]^+$ cations and PF_6^- ions. In contrast, neighboring molecules in **2** are linked into a supramolecular chain structure through aromatic stacking interactions between two $dfppy^-$ ligands. In solution, **1·PF$_6$** and **2** show acid/base-induced structural transformation due to the protonation/deprotonation of their pyridyl groups and/or imidazole units, which can be confirmed by their ^{1}H NMR spectra. At room temperature, compounds **1·PF$_6$**, **2** and pidpyH in CH_2Cl_2 reveal TFA-induced luminescence switching behaviors, from non-luminescence state to a luminescence state with an emission at 582 nm for both **1·PF$_6$** and **2**, and emission switching from 392 nm to 502 nm for pidpyH. These switching behaviors are associated with the protonation of pyridyl groups and/or imidazole units in **1·PF$_6$**, **2** and pidpyH (Scheme S6). Moreover, compounds **1·PF$_6$** and **2** were used as photosensitizers (PS) for reducing water to hydrogen under the same experimental condition. It was found that the amount of evolved hydrogen and the PS turnover number are respectively 512 μmol and 102 for **1·PF$_6$**, and 131 μmol and 26 for **2**. Thus, compound **1·PF$_6$** has better photocatalytic activity than **2**. In this paper, we discuss the modulation of luminescence and photocatalytic activities of **1·PF$_6$** and **2** by varying the coordination mode and/or protonation extent of pidpyH/$pidpy^-$ ligands.

Introduction

Cyclometalated Ir(III) complexes are being explored because of their potential applications in chemosensors,[1] phosphorescent emitters in organic light-emitting diodes (OLEDs),[2] cellular imaging,[3] information storage and security protection,[4] and catalysis[5] *etc*. The structures and related functional properties of cyclometalated Ir(III) complexes can be modulated through incorporating various C^N ligands, for example 2-phenyl-pyridine and its derivatives, and/or ancillary ligands, such as 2,2'-bipyridine,[6] 1,10-phenanthroline,[7] acetylacetonate,[8] picolinate,[9] and their derivatives,[10] *etc*. It should be noted that based on an imidazole-based N^N ancillary ligand, a pair of proton-switchable cyclometalated Ir(III) complexes could be obtained, in which their imidazole units coordinate to Ir(III) ion through neutral –N= donor and deprotonated -N$^-$- donor, respectively, thus showing different luminescence behaviors. For example, in 2010, Hallett, Pope, *et al.* reported the crystal structures of $[Ir(ppy)_2(L^1)]$ and $[Ir(ppy)_2(LH^1)][PF_6]$ (Scheme S1),[11] in which the imidazole units of L^1 and LH^1 ligands show deprotonation and protonation state, respectively. In CH_3CN, the former reveals weak luminescence, but strong luminescence at 560 nm for the latter. In the same year, Williams group reported complexes $[Ir(ppy)_2(pybz)]$ and $[Ir(ppy)_2(pybzH)]PF_6$ (Scheme S2),[12] in which the ancillary ligands $pybz^-$ and pybzH adopt N^N$^-$ and N^N coordination mode, respectively. In CH_2Cl_2, the former shows the phosphorescence at 496 and 521 nm, while 590 nm for the latter. The DCl/NaOD-induced structural interconversion (*i.e.* proton-switchable behavior, seeing Scheme S2) of two complexes was confirmed by their ^{1}H NMR spectra, but no related crystal structure was reported. Recently, the others cyclometalated Ir(III) complexes were also obtained based on some imidazole-based N^N ancillary ligands (Scheme S3),[13] in which their proton-switchable behaviors can result in the significant variation in electronic absorption spectra,[15a] luminescence intensity,[13b,d] and emission color.[13c,d] Moreover, Yu, *et. al.* synthesized five $BiBzImH_2$-based cyclometalated Ir(III) complexes (Scheme S4), and used these mono/di-nuclear iridium compounds as photosensitizers for photocatalytic reduction of water to hydrogen.[5d] It was found that the photocatalytic activities of these dinuclear iridium compounds are better than the activities of their mononuclear analogues, which is probably associated with relatively intense absorption within visible light range for these dinuclear compounds. So far, the number of imidazole-based cyclometalated Ir(III) complexes is still limited. Thus more cases are necessary to be prepared in order to further explore their acid/base-induced structural transformation and related functional properties such as luminescence and photocatalytic activity.

In this paper, we synthesized the imidazole-based ligand pidpyH (Scheme 1), which contains an imidazole unit and two pyridyl groups. Based on pidpyH and 2-(2,4-difluorophenyl)-pyridine (dfppyH), two cyclometalated Ir(III) complexes $[Ir(dfppy)_2(pidpyH)](PF_6)$ **(1·PF$_6$)** and $[Ir(dfppy)_2(pidpy)]$ **(2)** were prepared, with the below two main aims. (1) Each $\{Ir(dfppy)_2\}^+$ unit is coordinated by a neutral ligand pidpyH through N,N-chelating mode (Scheme S5) in **1·PF$_6$**, while a $pidpy^-$ anion through N,N$^-$-chelating mode in **2**. We can thus explore the influence of the structural difference between **1·PF$_6$**

View Article Online
DOI: 10.1039/C7DT01337J

and **2** on their luminescence behaviors and photocatalytic activities for hydrogen evolution. (2) In **1·PF$_6$** and **2** (Figs. 3 and 4), ligands pidpyH/pidpy$^-$ contain imidazole units and non-coordinated pyridyl groups, which can be protonated/deprotonated by acid/base. This allows us to explore the influence of protonation/deprotonation of pidpyH/pidpy$^-$ ligand on the luminescence behaviors of **1·PF$_6$** and **2**. In addition, control compounds [Ir(dfppy)$_2$(pidpyH)]Cl (**1·Cl**) and [Ir(dfppy)$_2$(pidpyH$_2$)]2Cl (**1H·2Cl**) were also prepared (seeing their molecular structures and synthesis details in ESI) in order to study the acid/base-induced structural transformation and luminescence behaviors of **1·PF$_6$** and **2**. Herein, we report the crystal structures of **1·PF$_6$** and **2**, acid/base-induced structural transformation and luminescence switching, and photocatalytic activity for hydrogen evolution.

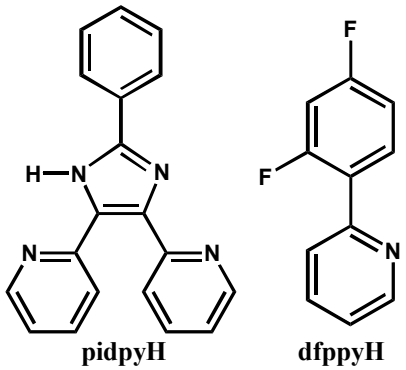

pidpyH **dfppyH**

Scheme 1

Experimental

Materials and methods

Compounds 2,2'-(2-phenyl-1H-imidazole-4,5-diyl)dipyridine (pidpyH) and [Ir(dfppy)$_2$Cl]$_2$ dimer were prepared according to the literature methods.[14] All other reagents were commercially available and used without further purification. Elemental analyses were performed on a Perkin Elmer 240C elemental analyzer. The IR spectra were obtained as KBr disks on a VECTOR 22 spectrometer. The ^{1}H NMR spectra were recorded at room temperature with a 300 or 400 MHz BRUKER spectrometer. UV-vis absorption spectra were measured on a Cary 100 spectrophotometer. The luminescence spectra at room temperature and at 77 K were measured on a Hitachi F-4600 fluorescence spectrometer. The solid-state luminescence spectra were measured using a Perkin Elmer LS55 fluorescence spectrometer. The luminescence lifetimes and photoluminescence quantum yields of solid-state samples were measured at room temperature on an Edinburgh FL-FS920 fluorescence spectrometer. The photoluminescence quantum yields of **1·PF$_6$**, **2** and pidpyH in CH_2Cl_2 were measured by a relative method by comparison with a standard, a solution of quinine sulfate in 0.5 M H_2SO_4 (Φ = 54.6%, λ_{ex} = 366 nm).[13d]

Hydrogen evolution

The hydrogen evolution experiment was carried out in a Pyrex vessel with an irradiation light source of 300 W xenon lamp, as described previously.[5d] All samples were dissolved in 200 mL of CH_3CN-H_2O (v/v = 4/1) mixture, including **1·PF$_6$** or **2** (50 μM, photosensitizer), K_2PtCl_4 (0.1 mM, electron relay) and triethanolamine (0.1 M, sacrificial reductant). The wavelength of irradiation light is ≥410 nm. Before light irradiation, the system was evacuated successively before being backfilled with argon. The evolved gas was periodically detected on a gas chromatograph equipped with a thermally conductive detector (Shimadzu GC-8A, argon as a carrier gas and MS-5A column).

Synthesis of [Ir(dfppy)$_2$(pidpyH)](PF$_6$) (1·PF$_6$)

A mixture of pidpyH (0.2 mmol, 0.0629 g) and [Ir(dfppy)$_2$Cl]$_2$ (0.1 mmol, 0.1216 g) in CH_2Cl_2-CH_3OH (v/v = 5/4) (27 mL) was heated in an oil bath (50 ^{o}C) under argon for one day. After evaporation under vacuum, the resultant residue was dissolved in a mixture of CH_2Cl_2 (30 mL) and saturated KPF_6 aqueous solution (20 mL). This mixture was vigorously stirred for two hours, and then extracted with CH_2Cl_2 (30 mL × 2). The combined CH_2Cl_2 solution was dried with $MgSO_4$, filtered, and then evaporated. The resultant residue was purified through silica column chromatography using CH_3OH-CH_2Cl_2 (v/v = 0-3/100) solution, obtaining a yellow solid. Yield: 144 mg, 71% based on [Ir(dfppy)$_2$Cl]$_2$. Anal. found (calcd) for $C_{41}H_{26}F_{10}N_6PIr$: C, 48.57 (48.48); H, 2.72 (2.58), N, 8.12 (8.27). IR (KBr, cm^{-1}): 3393(w), 3104(w), 1605(s), 1575(s), 1479(s), 1429(m), 1405(s), 1295(m), 1267(w), 1249(w), 1223(w), 1165(w), 1117(w), 1104(m), 989(m), 844(s), 785(w), 758(w), 712(w), 698(s), 558(m), 526(w). ^{1}H NMR (400 MHz, $CDCl_3$), δ (ppm): 5.23 and 5.25 (d, 1H), 5.60 and 5.62 (d, 1H), 6.11 (t, 1H), 6.50 (t, 1H) [5.23-6.50 ppm: total 4H from two 2,4-difluorophenyl rings of the dfppy$^-$ units], 6.99-7.07 (m, 5H from the phenyl group of pidpyH ligand), 7.16-7.23 (2t, 2H), 7.33 (t, 1H), 7.44 (t, 1H), 7.65(d, 1H) and 7.75(d, 1H) [7.16-7.23 and 7.33-7.75 ppm: total 6H from two pyridyl rings of the dfppy$^-$ units], 7.82 (m, 3H), 8.01 (t, H), 8.14 and 8.16 (2d, 2H) [7.82-8.16 pm: total 6H from two pyridyl groups of pidpyH ligand), 8.23-8.28 (2d, 2H from two pyridyl rings of the dfppy$^-$ units), 8.74 and 8.76 (2d, 2H from two pyridyl groups of pidpyH ligand).

Synthesis of [Ir(dfppy)$_2$(pidpy)] (2)

A mixture of pidpyH (0.2 mmol, 0.0629 g), [Ir(dfppy)$_2$Cl]$_2$ (0.1 mmol, 0.1216 g) and K_2CO_3 (0.6 mmol, 0.0825 g) in CH_2Cl_2-CH_3OH (v/v = 5/4) (27 mL) was heated in an oil bath (50 ^{o}C) under argon for one day. After evaporation under vacuum, the resultant residue was mixed with H_2O (10 mL), and then the mixture was extracted with CH_2Cl_2 (25 mL × 3). The combined CH_2Cl_2 solution was dried with $MgSO_4$, filtered, and then evaporated. The resultant residue was purified through silica column chromatography using CH_3OH-CH_2Cl_2 (v/v = 0-3/100) solution, obtaining a yellow solid. Yield: 108 mg, 60% based on [Ir(dfppy)$_2$Cl]$_2$.

Compound **2** can also be synthesized by the reaction of compound **1·PF$_6$** and NaOH using the below procedure. To a solution of compound **1·PF$_6$** (0.035 mmol, 0.0355 g) in CH_2Cl_2 (10 mL) was added an aqueous solution of NaOH [3 mL, containing NaOH (0.35 mmol, 0.0140 g)]. This mixture was vigorously stirred at room temperature for 24 hours. After the separation of the CH_2Cl_2 layer, the H_2O layer was extracted with CH_2Cl_2 (15 mL × 2). The combined CH_2Cl_2 solution was dried with $MgSO_4$, filtered, and then evaporated, obtaining yellow solid

View Article Online
DOI: 10.1039/C7DT01337J

of **2**. Yield: 31 mg, 97% based on compound **1·PF$_6$**. Anal. found (calcd) for $C_{41}H_{25}N_6F_4Ir$: C, 56.76 (56.61); H, 3.05 (2.90), N, 9.81 (9.66). IR (KBr, cm^{-1}): 3127(m), 2973(w), 1604(s), 1571(w), 1557(w), 1535(w), 1477(m), 1401(s), 1292(w), 1247(w), 1228(w), 1162(w), 1100(w), 1048(w), 986(w), 850(w), 826(w), 813(w), 784(w), 701(w). ^{1}H NMR (400 MHz, $CDCl_3$), δ (ppm): 5.20 and 5.22 (d, 1H), 5.65 and 5.66 (d, 1H), 6.09 (t, 1H), 6.44 (t, 1H) [5.20-6.44 ppm: total 4H from two 2,4-difluorophenyl rings of the dfppy$^-$ units], 6.88-7.23 (m, total 9H: 5H from the phenyl group of pidpyH ligand and 4H from two pyridyl rings of the dfppy$^-$ units), 7.63-7.84 (m, 6H), 8.05 (d, 1H), 8.19 (2t, 2H) and 8.32(d, 1H) [7.63-7.84 pm: total 10H: 6H from two pyridyl groups of pidpyH ligand and 4H from two pyridyl rings of the dfppy$^-$ units], 8.68 and 9.30 (2d, 2H from two pyridyl groups of pidpyH ligand).

Table 1 Crystallographic data and refinement for **1·PF$_6$** and **2**

	1·PF$_6$	**2**
Formula	$C_{41}H_{26}F_{10}IrN_6P$	$C_{41}H_{25}F_4IrN_6$
M	1015.85	869.87
Crystal system	Triclinic	Monoclinic
Space group	$P\bar{1}$	$C2/c$
T /K	296	296
a /Å	10.1303(6)	21.8943(8)
b /Å	13.8487(8)	24.2539(9)
c /Å	14.4314(9)	13.4991(5)
α / °	84.7650(10)	
β /°	78.8280(10)	93.3900(10)
γ / °	70.7100(10)	
V/Å^3	1873.92(19)	7155.8(5)
Z	2	8
D_c /g cm^{-3}	1.800	1.615
F(000)	992	3408
GooF on F^2	1.038	1.034
R_1, wR_2 [$I>2\sigma(I)$]^a	0.0343, 0.0678	0.0198, 0.0605
R_1, wR_2 (all data)^a	0.0420, 0.0708	0.0232, 0.0625
$(\Delta\rho)_{max}$, $(\Delta\rho)_{min}$ (e Å^{-3})	0.720, -0.598	1.169, -0.827

^{a} $R_1 = \Sigma||F_o|-|F_c||/\Sigma|F_o|$. $wR_2=[\Sigma w(F_o^2-F_c^2)^2/\Sigma w(F_o^2)^2]^{1/2}$.

Table 2 Selected bond lengths (Å) and bond angles (°) for **1·PF$_6$**

Ir1-C1	2.018(5)	Ir1-N3	2.148(4)
Ir1-C12	2.011(5)	Ir1-N5	2.165(4)
Ir1-N1	2.047(4)	N4-C35	1.350(6)
Ir1-N2	2.039(4)	N5- C35	1.323(6)
C1-Ir1-C12	84.07(18)	N2-Ir1-N3	85.49(15)
C1-Ir1-N1	79.99(18)	N2-Ir1-N5	95.80(15)
C1-Ir1-N2	96.98(18)	N3-Ir1-N5	75.94(14)
N1-Ir1-N2	176.33(14)	C12-Ir1-N2	80.05(18)
C1-Ir1-N3	177.21(18)	C12-Ir1-N1	97.49(18)
C1-Ir1-N5	105.02(16)	C12-Ir1-N3	95.12(16)
N1-Ir1-N3	97.49(15)	C12-Ir1-N5	170.49(17)
N1-Ir1-N5	87.03(15)		

Table 3 Selected bond lengths (Å) bond angles (°) for **2**

Ir1-C1	2.010(2)	Ir1-N3	2.1493(19)
Ir1-C12	2.001(2)	Ir1-N4	2.1524(18)
Ir1-N1	2.0416(19)	N4-C35	1.359(3)
Ir1-N2	2.0425(19)	N5- C35	1.333(3)
C1-Ir1-C12	84.66(9)	N2-Ir1-N3	85.37(7)
C1-Ir1-N1	80.48(9)	N2-Ir1-N4	99.46(7)
C1-Ir1-N2	94.65(9)	N3-Ir1-N4	76.04(7)
N1-Ir1-N2	174.70(7)	C12-Ir1-N1	96.79(8)
C1-Ir1-N3	179.71(8)	C12-Ir1-N2	80.58(8)
C1-Ir1-N4	104.24(8)	C12-Ir1-N3	95.07(8)
N1-Ir1-N3	99.49(7)	C12-Ir1-N4	171.05(7)
N1-Ir1-N4	83.86(7)		

X-Ray crystallographic studies

The yellow blocky crystals of **1·PF$_6$** and **2** were obtained through evaporation of a $CHCl_3$-CH_3OH solution for **1·PF$_6$**, and a $CH_3COOC_2H_5$-CH_3OH solution for **2**. Single crystals of dimensions 0.28 × 0.18 × 0.15 mm^3 for **1·PF$_6$**, and 0.23 × 0.20 × 0.16 mm^3 for **2** were used for structural determination on a Bruker SMART APEX CCD diffractometer using graphite-monochromated Mo Kα radiation (λ = 0.71073 Å) at room temperature. A hemisphere of data were collected in the θ range 1.44 to 25.00° for **1·PF$_6$**, and 2.69 to 27.53° for **2** using a narrow-frame method with scan widths of 0.30° in ω and an exposure time of 10 s per frame. Numbers of observed and unique reflections are 10534 and 6517 (R_{int} = 0.0300) for **1·PF$_6$**, and 31486 and 8195 (R_{int} = 0.0234) for **2**, respectively. The data were integrated using the Siemens *SAINT* program,[15] with the intensities corrected for Lorentz factor, polarization, air absorption, and absorption due to variation in the path length through the detector faceplate. Multi-scan absorption corrections were applied. The structures were solved by direct methods and refined on F^2 by full matrix least squares using *SHELXTL*.[16] All the non-hydrogen atoms were located from the Fourier maps, and were refined anisotropically. All H atoms were refined isotropically, with the isotropic vibration parameters related to the non-H atom to which they are bonded. In the structural refinement of **2**, a region of disordered electron density, probably some disordered $CH_3COOC_2H_5$ molecules, was treated using the SQUEEZE routine in *PLATON*. For compound **2**, the given chemical formula and crystal data do not take into account these solvent molecules. In addition, some disagreeable reflections were omitted in the structural refinement of both **1·PF$_6$** and **2**. These refinement details can be found in the cif files containing the information of hkl and res files. The crystallographic data for compounds **1·PF$_6$** and **2** are listed in Table 1, and selected bond lengths and bond angles are given in Tables 2 and 3. CCDC 1550506 and 1550507 contain the supplementary crystallographic data of **1·PF$_6$** and **2**, respectively, which can be obtained free of charge from the Cambridge Crystallographic Data Centre via www.ccdc.cam.ac.uk/data_request/cif.

Results and discussion

Syntheses and acid/base-induced structural transformation

Compound **1·PF$_6$** was synthesized through stirring the mixture of pidpyH and $[Ir(dfppy)_2Cl]_2$ in CH_2Cl_2-CH_3OH solution at 50 °C for 24 hours, and an anion exchange of Cl^- by using PF_6^-. In contrast, compound **2** was prepared through the reaction of pidpyH, $[Ir(dfppy)_2Cl]_2$ and K_2CO_3, or by a deprotonation reaction of **1·PF$_6$** in a mixture of CH_2Cl_2 and aqueous solution of NaOH. Therefore, **1·PF$_6$** and **2** show distinctly different structures. An $\{Ir(dfppy)_2\}^+$ unit is chelated by a pidpyH ligand in **1·PF$_6$**, but a pidpy$^-$ anion in **2**, which is

View Article Online
DOI: 10.1039/C7DT01337J

confirmed by their crystal structures (Figs. 3 and 4). Additionally, both **1·PF$_6$** and **2** reveal acid/base-induced structural transformation. After the $CDCl_3$ solution of **1**·PF_6 was fully mixed with a D_2O solution of NaOH, its ^{1}H NMR spectrum is almost the same as that of **2** (Figs. 1, S2, S3 and S6), indicating the structural transformation from **1·PF$_6$** to compound **2**. It was found that the

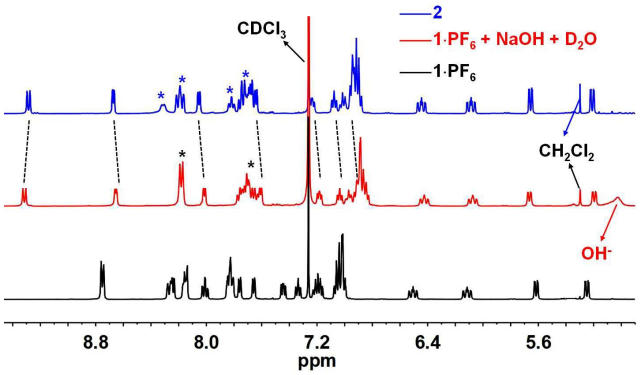

Fig. 1 The ^{1}H NMR spectrum of **1·PF$_6$** after adding a D_2O solution of NaOH, and the ^{1} H NMR spectra of **1·PF$_6$** and **2** (dotted line indicating position variations, signals with * occurring separation/combination).

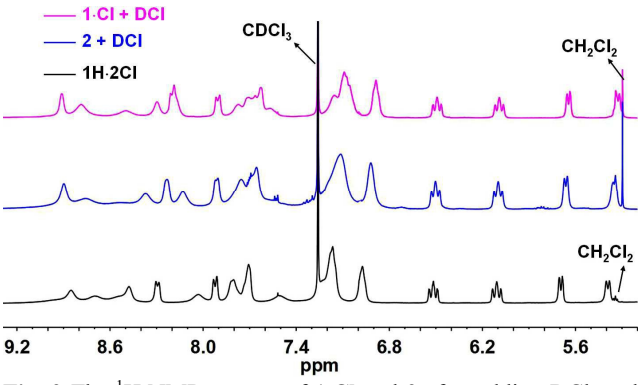

Fig. 2 The ^{1}H NMR spectra of **1·Cl** and **2** after adding DCl, and the ^{1} H NMR spectrum of **1H·2Cl**.

^{1}H NMR spectra of "**1**·PF_6+NaOH+D_2O" and **2** reveal the following two minor differences. (1) Two signals at 7.60-7.77 ppm and 8.19 ppm in "**1**·PF_6+NaOH+D_2O" changed to four separated signals at 7.63-7.84 ppm and 8.19-8.32 ppm in **2** (seeing the signals with * in Fig. 1). (2) Some corresponding signals in "**1**·PF_6+NaOH+D_2O" and **2** show slight position variation (seeing the signals connected by dotted lines in Fig. 1). These differences could be mainly assigned to the influence of PF_6^- anion in "**1**·PF_6+NaOH+D_2O" mixture, which is confirmed by the different ^{1}H NMR spectra between **1**·PF_6 and **1**·Cl (Figs. S2, S4 and S9). After adding some DCl in the $CDCl_3$ solution of **2**, although the measured ^{1}H NMR spectrum is different from that of **1H·2Cl** due to the influence of excess DCl, it is in agreement with the ^{1}H NMR spectrum of "**1·Cl**+DCl" (Figs. 2, S5, S7 and S8, seeing the molecular structures of **1H·2Cl** and **1·Cl** in ESI). This indicates that the pidpy$^-$ ligand in compound **2** underwent DCl-induced structural changes, including the protonation of non-coordinated pyridyl ring and the coordination-mode transition from N,N$^-$-chelating mode to N,N−chelating mode (Scheme S5).

It should be noted that the addition of DCl in the $CDCl_3$ solution of **1·PF$_6$** immediately resulted in some solid. Thus, the ^{1}H NMR spectrum of "**1·PF$_6$**+DCl" has not been measured. The ^{1}H NMR experiments indicate that both **1·PF$_6$** and **2** showed acid/base-induced structural transformation, which would lead to their luminescence switching in solution.

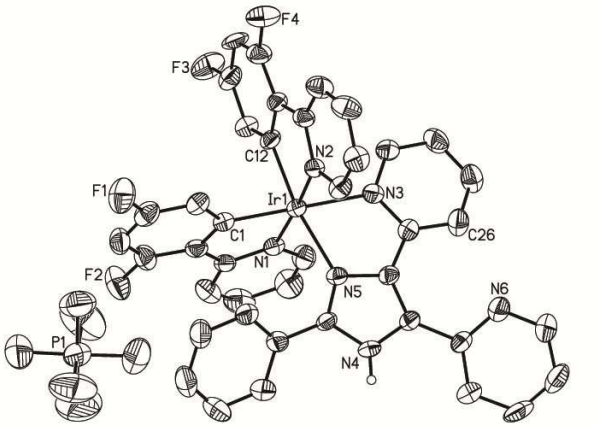

Fig. 3 Molecular structure of **1·PF$_6$**. All H atoms attached to C atom are omitted for clarity.

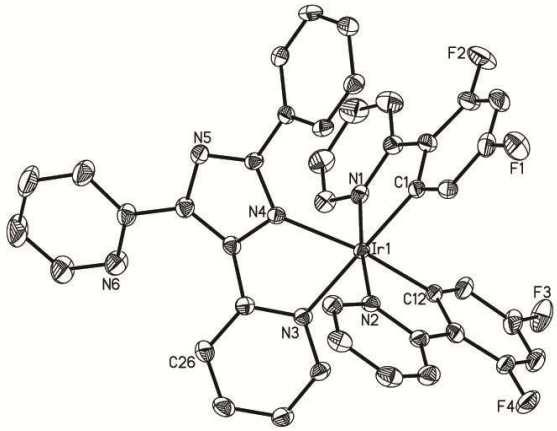

Fig. 4 Molecular structure of **2**. All H atoms attached to C atom are omitted for clarity.

Crystal structures of 1 and 2

Compounds **1·PF$_6$** and **2** crystallize in the triclinic space group $P\bar{1}$ and monoclinic space group $C2/c$, respectively. In the molecular structure of **1·PF$_6$** (Fig. 3), a neutral pidpyH ligand coordinates to an $\{Ir(dfppy)_2\}^+$ unit through N,N-chelating mode (Scheme S5), and the resultant cationic unit $[Ir(dfppy)_2(pidpyH)]^+$ and its counter ion PF_6^- are held together by electrostatic interaction. Compared to **1·PF$_6$**, compound **2** is a neutral complex (Fig. 4), in which an $\{Ir(dfppy)_2\}^+$ unit is coordinated by a pidpy$^-$ anion through N,N$^-$-chelating mode (Scheme S5). Each Ir(III) ion in **1·PF$_6$** and **2** shows a distorted octahedral coordination geometry. Four of the six coordination sites are occupied by two pyridine nitrogen atoms (N1, N2) and two carbon atoms (C1 and C12) from two nonequivalent cyclometallated dfppy$^-$ ligands. The remaining two coordination sites are occupied by two nitrogen atoms from a pidpyH/pidpy$^-$ ligand (N3 and N5 in **1·PF$_6$**, N3 and N4 in **2**). Around each Ir(III) ion, the Ir-C(N) distances are in the

View Article Online
DOI: 10.1039/C7DT01337J

range 2.011(5)-2.165(4) Å in **1·PF$_6$**, and 2.001(2)-2.1524(18) Å in **2**. It should be noted that Ir-N$_{imidazole}$ bond length in **1·PF$_6$** [Ir1-N5 = 2.165(4) Å] is significantly longer than that in **2** [Ir1-N4 = 2.1524(18) Å], due to the fact that the imidazole nitrogen atom N5 in **1·PF$_6$** has weaker basicity than that of the deprotonated N4 atom in **2**.[13b]

In **1·PF$_6$** and **2**, two cyclometallated dfppy$^-$ ligands around each Ir(III) adopt the same *C,C-cis* and *N,N-trans* configurations as those in [Ir(dfppy)$_2$Cl]$_2$.[17] The ancillary ligands pidpyH/pidpy$^-$ are arranged with their coordinated nitrogen atoms (N3 and N5 in **1·PF$_6$**, N3 and N4 in **2**) lying in a position trans to the corresponding σ-bound carbon atoms (C1 and C12) in the dfppy$^-$ ligands. Therefore, the Ir–N3/N4/N5 bond lengths [2.148(4)–2.165(4) Å] in **1·PF$_6$** and **2** are significantly longer than Ir–C/N1/N2 bond distances [2.001(2)–2.047(4) Å].[18] In **1·PF$_6$** and **2**, both pidpyH and pidpy$^-$ ligands show similar intra-ligand hydrogen bond interaction [seeing Fig.3, C26-H···N6 = 3.023(1) Å in **1·PF$_6$** and 3.022(1) Å in **2**].[19] However, ligands pidpyH and pidpy$^-$ in **1·PF$_6$** and **2** reveal different twist extent, which was confirmed by their dihedral angles among imidazole ring, phenyl ring, coordinated pyridyl ring and noncoordinated pyridyl ring [in **1·PF$_6$**: 46.7(1)^o between imidazole ring and phenyl ring, 4.7(1)^o between imidazole ring and coordinated pyridyl ring, and 29.9(1)^o between imidazole ring and noncoordinated pyridyl ring; in **2**: the corresponding dihedral angles showing 36.4(1)^o, 26.2(1)^o and 12.7(1)^o, respectively].

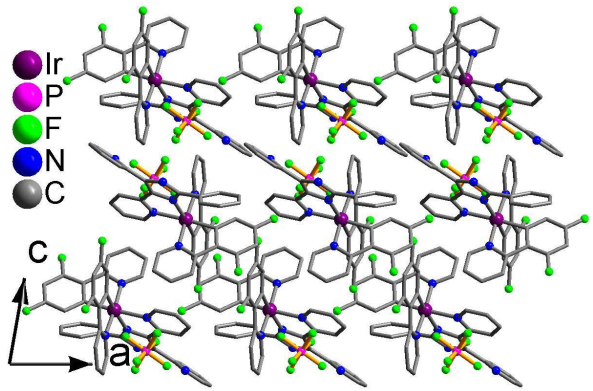

Fig. 5 The packing structure of **1·PF$_6$**. All H atoms are omitted for clarity.

Clearly, compounds **1·PF$_6$** and **2** show distinct molecular structures. In addition, two compounds reveal significantly different packing structures. As shown in Fig. 4, neighboring [Ir(dfppy)$_2$(pidpyH)]$^+$ cations in **1·PF$_6$** stack only through van der Waals interactions, and inter-cation space is filled with PF_6^- ion. In contrast, neighboring [Ir(dfppy)$_2$(pidpy)] molecules in **2** are linked into a supramolecular chain structure along *c* axis (Fig. 5) through aromatic stacking interactions between two dfppy$^-$ ligands from adjacent molecules [the plan···plan distance between pyridine ring and difluorophenyl ring: around 3.350(1) Å].[20] These chains are held together by van der Waals interactions (Fig . S12).

Electronic absorption spectra

The UV-vis spectra of pidpyH, **1·PF$_6$**, and **2** were measured in CH_2Cl_2 at room temperature (Table S1). Compound pidpyH shows two broad $\pi\rightarrow\pi^*$ absorption bands around 233 nm and 260-375 nm, respectively (Fig. 6). Compared to pidpyH, compounds **1·PF$_6$** and **2** reveal wider UV-vis absorption, including high-energy absorption bands (around 249 nm and 305 nm for **1·PF$_6$**, and around 257 nm and 303 nm for **2**), and low-energy absorption band in the range 361-430 nm. The high-energy absorption bands of **1·PF$_6$** and **2** could be assigned to spin-allowed ligand-centered (^{1}LC) transitions (dfppy$^-$ and pidpyH/pidpy$^-$ ligands). In these low-energy absorption bands of **1·PF$_6$** and **2**, the bands around 373 nm is likely to be a combination of spin-allowed metal-to-ligand charge transfer (^{1}MLCT) and ligand-centered (^{1}LC) transitions, because of the high extinction coefficient ($\varepsilon = 1.03 \times 10^4$ M^{-1} cm^{-1} in **1·PF$_6$**, and $\varepsilon = 2.22 \times 10^4$ M^{-1} cm^{-1} in **2**).[21,13b,d] The weaker absorption tail towards 430 nm is mainly attributed to spin-forbidden ^{3}MLCT absorption.[22] Moreover, compounds **1·PF$_6$** and **2** exhibit significantly different absorption intensity around 305 nm and 373 nm (Fig.6), due to their different ancillary ligands (pidpyH in **1·PF$_6$**, while pidpy$^-$ in **2**).

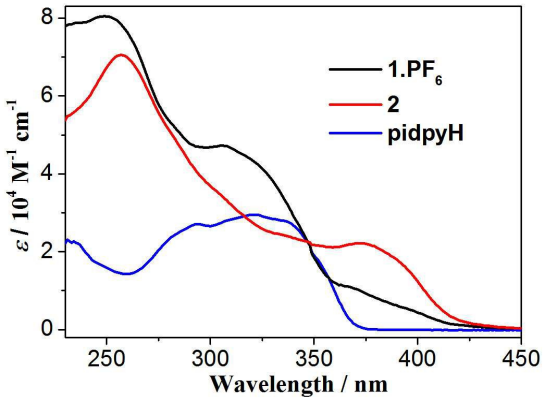

Fig. 6 UV-vis absorption spectra of compounds pidpyH, **1·PF$_6$** and **2** in CH_2Cl_2.

Luminescence properties

The luminescence spectra of pidpyH, **1·PF$_6$** and **2** were measured in CH_2Cl_2 at room temperature, using excitation light at 332 nm for pidpyH, and 377 nm for **1·PF$_6$** and **2**. Compound pidpyH shows an emission at 392 nm (Fig. S14). In contrast, compounds **1·PF$_6$** and **2** are weakly luminescent or non-luminescent. This could be due to some temperature-dependent non-radiative processes,[23] which is confirmed by the fact that both **1·PF$_6$** and **2** show gradual decrease in luminescence intensity upon increasing the temperature from 77 K to room temperature (Figs. S15 and S16). At 77 K, the strong luminescence of **1·PF$_6$** and **2** could be assigned to the enhanced rigidity of molecules, which can effectively diminish the loss of energy in the nonradiation decay process.[24]

Considering the pyridyl groups and imidazole units of ligands pidpyH/pidpy$^-$ can be protonated by TFA, We measured the luminescence behaviors of compounds pidpyH, **1·PF$_6$** and **2** at room temperature after adding TFA in their CH_2Cl_2 solutions. Upon gradual addition of TFA from 0.5 to 6.5 eq., the 392 nm emission of pidpyH gradually decreased in luminescence intensity (Fig. 7), and a new emission at 502 nm was observed

View Article Online
DOI: 10.1039/C7DT01337J

Table 4 Photophysical properties of **1·PF$_6$** and **2** in CH_2Cl_2 and in solid state

Compound	Medium (T [K])	λ_{abs} [nm] (M^{-1} cm^{-1})	λ_{em} [nm]	Lifetime	quantum yield
pidpyH	CH_2Cl_2 (298)	233, 360–375	389	10.7 μs and 1.7 μs	9.3%
	CH_2Cl_2 (77K)	-	383， 404	-	-
pidpyH+TFA	CH_2Cl_2 (298)	-	502	11.1 μs and 1.9 μs	9.9%
	CH_2Cl_2 (77K)	-	400	-	-
1·PF$_6$	CH_2Cl_2 (298)	249, 305, 361–430	-	-	-
	CH_2Cl_2 (77K)	-	515， 546	-	-
	Solid (298)	-	485， 532	2512 ns and 411 ns	1.8%
1·PF$_6$ + TFA	CH_2Cl_2 (298)	-	582	658 ns and 308 ns	2.8%
	CH_2Cl_2 (77K)	-	499， 528	-	-
2	CH_2Cl_2 (298)	257, 303, 361–430	-	-	-
	CH_2Cl_2 (77K)	-	515， 546	-	-
	Solid (298)	-	486， 530， 571	1758 ns and 324 ns	0.5%
2 + TFA	CH_2Cl_2 (298)	-	582	548 ns and 251 ns	2.9%
	CH_2Cl_2 (77K)	-	499， 528	-	-

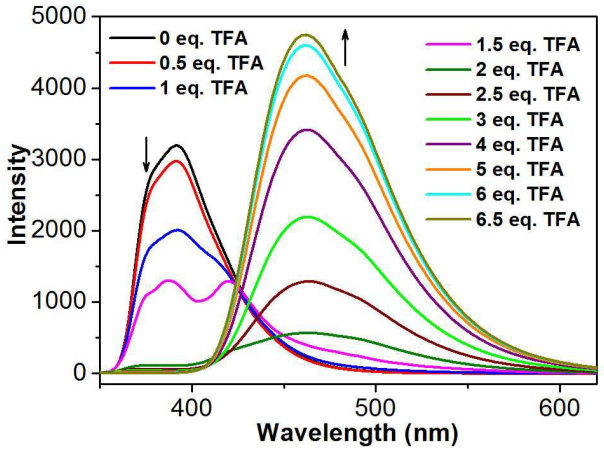

Fig. 7 Luminescence spectra1 changes of pidpyH in CH_2Cl_2 (c = 1 × 10^{-4} M, λ_{ex} = 332 nm) upon adding TFA.

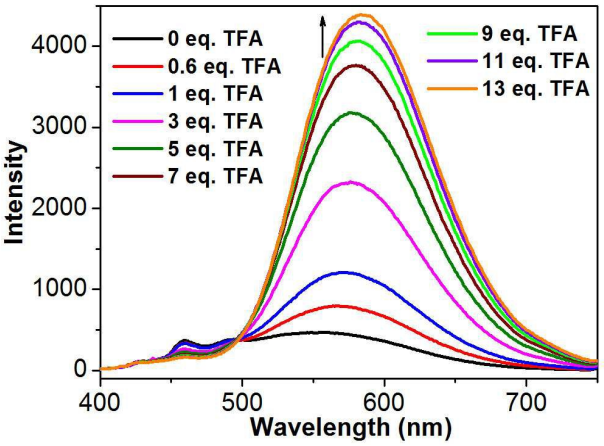

Fig. 8 Luminescence spectral changes of **1·PF$_6$** in CH_2Cl_2 (c = 1 × 10^{-4} M, λ_{ex} = 377 nm) upon adding TFA.

due to the formation of $[pidpyH_4]^{3+}$ specie (Scheme S6). After addition of excess TFA, compounds **1·PF$_6$** and **2** revealed the same strong emission at 582 nm (Figs. 8 and 9), which is assigned to the formation of the same $\mathbf{[1H]^{2+}}$ specie resulted from TFA-induced structural transformation of **1·PF$_6$** and **2** (Scheme

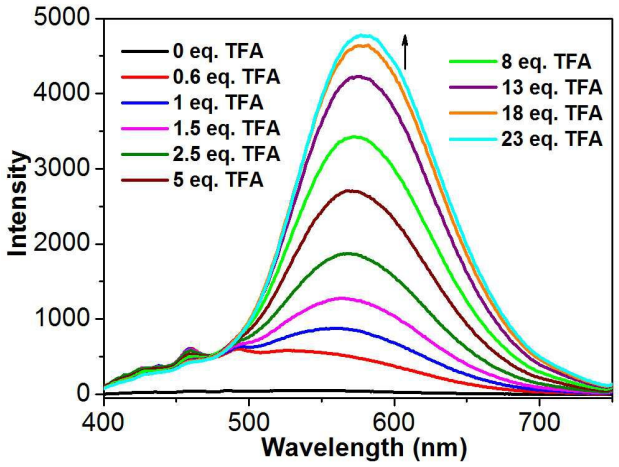

Fig. 9 Luminescence spectral changes of **2** in CH_2Cl_2 (c = 1 × 10^{-4} M, λ_{ex} = 377 nm) upon adding TFA.

S6). It should be noted that excess TFA needed to be added in order to observe the maximum luminescence intensity of pidpyH, **1·PF$_6$** and **2** (seeing Figs. 7-9, adding TFA about 6 eq., 11 eq. and 18 eq., respectively). This indicates that $[pidpyH_4]^{3+}$ and $\mathbf{[1H]^{2+}}$ species (Scheme S6) have deprotonation tendency in CH_2Cl_2, and excess TFA can restrain the deprotonation of $[pidpyH_4]^{3+}$ and $\mathbf{[1H]^{2+}}$, which is in agreement with the gradual increase in luminescence intensity of **1H·2Cl** upon addition of TFA from 2 to 12 eq (Fig. S17). In CH_2Cl_2-TFA mixture, we further measured the luminescence spectra of pidpyH, **1·PF$_6$** and **2** at 77 K (Fig. S18). The resultant $[pidpyH_4]^{3+}$ (from pidpyH+TFA) and $\mathbf{[1H]^{2+}}$ (from **1·PF$_6$**+TFA or **2**+TFA) show significantly blue-shifted emissions at 383 and 400 nm for $[pidpyH_4]^{3+}$, and 499 and 528 nm for $\mathbf{[1H]^{2+}}$, compared to the corresponding emissions at room temperature, *i.e.* 502 nm for "pidpyH+TFA", and 582 nm for both "**1·PF$_6$**+TFA" and "**2**+TFA". This significant rigidchromism is characteristic of a CT character for the luminescence of $[pidpyH_4]^{3+}$ and $\mathbf{[1H]^{2+}}$.[25] In addition, compounds pidpyH, **1·PF$_6$** and **2** can recover their original luminescence behaviors after adding some NEt_3 to neutralize the involved TFA (Figs. S19-S21). Therefore, compounds pidpyH, **1·PF$_6$** and **2** in CH_2Cl_2 can reversibly switch their luminescence behaviors upon alternately adding TFA and NEt_3, showing emission-wavelength switching

View Article Online
DOI: 10.1039/C7DT01337J

between 392 nm and 502 nm for pidpyH, and luminescence switching between off and on state for **1·PF$_6$** and **2**. The emission lifetimes of pidpyH, **1·PF$_6$** and **2** in CH_2Cl_2 were measured at room temperature (Table 4), and each one shows dual-exponential decay due to molecular aggregation in solution.[13b] The emission lifetimes are τ_1 = 10.7 μs (92.8% contribution) and τ_2 = 1.7 μs (7.2% contribution) for pidpyH, τ_1 = 11.1 μs (91.1% contribution) and τ_2 = 1.9 μs (8.9% contribution) for pidpyH after adding TFA, τ_1 = 658 ns (91.4% contribution) and τ_2 = 308 ns (8.6% contribution) for **1·PF$_6$** after adding TFA, and τ_1 = 548 ns (81.6% contribution) and τ_2 = 251 ns (20.4% contribution) for **2** after adding TFA (Table 4). Moreover, the luminescence quantum yields of pidpyH, **1·PF$_6$** and **2** in CH_2Cl_2 were measured at room temperature, obtaining Φ = 9.3% and 9.9%, respectively, for pidpyH before and after adding TFA, Φ = 2.8% for **1·PF$_6$** after adding TFA, and Φ = 2.9% for **2** after adding TFA (Table 4).

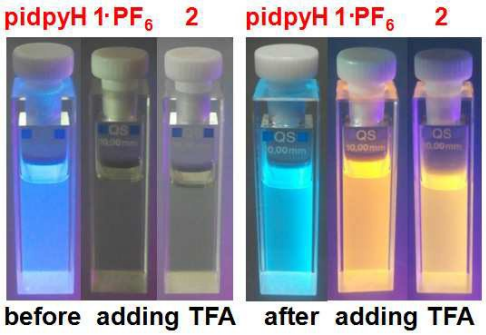

Fig. 10 The photographs of pidpyH, **1·PF$_6$** and **2** in CH_2Cl_2 under 365 nm light before and after adding TFA.

At room temperature, although compounds **1·PF$_6$** and **2** are weakly luminescent or non-luminescent in CH_2Cl_2, they are luminescent in solid state (Fig. S22). Compound **1·PF$_6$** reveals two strong and broad emissions at 485 nm and 532 nm, and **2** shows relatively weak luminescence with three broad emissions at 486 nm, 530 nm and 571 nm. The broad emissions of **1·PF$_6$** and **2** could be due to their molecular rigidity in solid state which can decrease nonradiation decay, and also because of inter-molecule stacking through van der Waals interactions and/or aromatic stacking interactions. The emission lifetimes are τ_1= 2512 ns (67% contribution) and τ_2 = 411 ns (33% contribution) for **1·PF$_6$**, and τ_1 = 1758 ns (81% contribution) and τ_2 = 324 ns for **2** (19% contribution). Their photoluminescence quantum yields in the solid state were Φ = 1.8% for **1·PF$_6$**, and Φ = 0.5% for **2** (Table 4).

Hydrogen evolution based on 1·PF$_6$ and 2

It is well known that some cyclometalated Ir(III) complexes can serve as efficient photosensitizers (PS) for photocatalytic reduction of water to hydrogen.[5a-d] In order to explore the influence of structural variation on the photocatalytic activity, hydrogen-evolution experiment was done using **1·PF$_6$** or **2** as photosensitizer. It was found that under the same experimental condition (seeing experiment section), the system containing **1·PF$_6$** produced 451 μmol of hydrogen after twelve-hour irradiation with λ ≥ 410 nm light (Fig. 11), while 118 μmol of hydrogen for **2**. After additional twelve-hour irradiation, the amount of hydrogen slowly increased to 512 μmol for **1·PF$_6$**, and 131 μmol for **2**. The reaction turnover numbers [TONs = n(H) / n(PS)][5d] were calculated according to one-electron transfer process, TON = 102 for **1·PF$_6$** and TON = 26 for **2**, indicating that **1·PF$_6$** has better photocatalytic activity than **2**. The significantly different photocatalytic activity between **1·PF$_6$** and **2** could be due to their distinct molecular structures. Each $\{Ir(dfppy)_2\}^+$ unit is coordinated by a neutral pidpyH ligand through N,N−chelating mode in **1·PF$_6$**, while by a pidpy$^-$ anion through N,N$^-$-chelating mode in **2** (Fig. 4 and Scheme S5). This possible structure-photocatalysis relationship provides a guiding principle for the design and fabrication of some imidazole-based Ir(III) complexes, which can serve as photosensitizers for reducing water to hydrogen. It should be noted that compounds **1·PF$_6$** and **2** show moderate/weak absorption in visible spectral region (Fig. 6), which is a drawback for their application in photocatalytic reduction of water to hydrogen. Thus, it is important for imidazole-based Ir(III) complexes to enhance their absorption in visible spectral region.

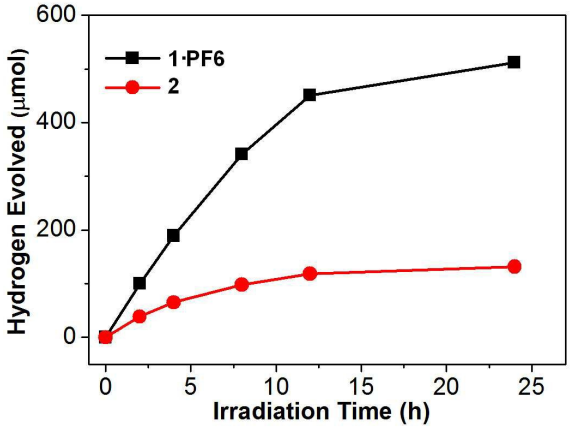

Fig. 11 Hydrogen evolution *vs.* irradiaton time plots, measured under the condition of using a light ($\lambda \geq 410$ nm) to irradiate a CH_3CN/H_2O (v/v = 4/1) solution containing **1·PF$_6$** or **2** (50 μM), K_2PtCl_4 (0.1 mM) and triethanolamine (0.1 M).

Conclusions

We have synthesized two new cyclometalated Ir(III) complexes $[Ir(dfppy)_2(pidpyH)](PF_6)$ **(1·PF$_6$)** and $[Ir(dfppy)_2(pidpy)]$ **(2)**. In the crystal structure of **1·PF$_6$**, each $\{Ir(dfppy)_2\}^+$ unit is coordinated by a neutral pidpyH ligand through N,N−chelating mode (Fig. 3 and Scheme S5), and these $\{Ir(dfppy)_2\}^+$ units and PF_6^- counter ions are held together through electrostatic interactions and van der Waals interactions. Compared to **1·PF$_6$**, each $\{Ir(dfppy)_2\}^+$ unit in **2** is coordinated by a pidpy$^-$ anion through N,N$^-$-chelating mode, and neighboring $[Ir(dfppy)_2(pidpy)]$ molecules are connected through aromatic stacking interactions, forming a supramolecular chain. The ^{1}H NMR experiment indicates that compounds **1·PF$_6$** and **2** show acid/base-induced structural transformation in solution, due to the protonation/deprotonation of their pyridyl groups and/or imidazole units. This structural transformation can result in the luminescence switching behaviors of **1·PF$_6$** and **2** in CH_2Cl_2. Both **1·PF$_6$** and **2** are non-luminescent. However, they reveal strong emission at 582 nm after adding TFA, which was assigned to the

View Article Online
DOI: 10.1039/C7DT01337J

formation of luminescent $[\mathbf{1H}]^{2+}$ specie (Scheme S6). Moreover, free pidpyH ligand can also reveal TFA-induced luminescence switching in CH_2Cl_2, from an emission at 392 nm to a red-shifted emission at 502 nm, which is due to the protonation of its pyridyl groups and imidazole unit. Therefore, compounds **1·PF$_6$**, **2** and pidpyH afford three examples of acid-responsive luminescent materials. Upon adding Et_3N to neutralize the involved TFA, compounds **1·PF$_6$**, **2** and pidpyH can recover their original emission behaviors. Additionally, compounds **1·PF$_6$** and **2** exhibit significantly different photocatalytic activity in the experiment of reducing water to hydrogen. After twenty-four-hour irradiation with $\lambda \geq 410$ nm light, the system containing **1·PF$_6$** produced 512 μmol of hydrogen, while 131 μmol of hydrogen for **2**. This indicates that **1·PF$_6$** has better photocatalytic activity than **2**, which could be due to the N,N−chelating mode of pidpyH ligand in **1·PF$_6$**. This structure-photocatalysis relationship needs to be further confirmed by more imidazole-based Ir(III) complexes. In this paper, our experimental results demonstrate that luminescence behaviors and photocatalytic activities of **1·PF$_6$** and **2** can be modulated by varying the coordination mode and/or protonation state of pidpyH/pidpy$^-$ ligands.

Acknowledgements

We acknowledge financial support from the NSF of Jiangsu Province, China (BK 20141314).

Notes

[a]*State Key Laboratory of Coordination Chemistry, Coordination Chemistry Institute, School of Chemistry and Chemical Engineering, Nanjing University, Nanjing 210093, P. R. China.*
Email: dkcao@nju.edu.cn
[b]*Department of Materials Science and Engineering Nanjing University, Nanjing 210093，P. R. China*

†Electronic Supplementary Information (ESI) available: Some synthesis details, Schemes and Tables, and some figures including ^{1}H NMR spectra, XRD pattern, crystal structure, UV-vis spectra, and luminescence spectra.

References

1 (*a*) H.-T. Cao, L. Ding, G.-G. Shan, H.-Z. Sun, Y. Wu and Z.-M. Su, *Dalton Trans.*, 2015, **44**, 19997; (*b*) M. Wang, K.-H. Leung, S. Lin, D. S.-H. Chan, D. W. J. Kwong, C.-H. Leung and D.-L. Ma, *Sci. Rep.*, 2014, **4**, 6794; (*c*) K. Y. Zhang, J. Zhang, Y. Liu, S. Liu, P. Zhang, Q. Zhao, Y. Tang and W. Huang, *Chem. Sci.*, 2015, **6**, 301; (*d*) Q. Zhao, X. Zhou, T. Cao, K. Y. Zhang, L. Yang, S. Liu, H. Liang, H. Yang, F. Li and W. Huang, *Chem. Sci.*, 2015, **6**, 1825; (*e*) J.-X. Ru, L.-P. Guan, X.-L. Tang, W. Dou, X. Yao, W.-M. Chen, Y.-M. Liu, G.-L. Zhang, W.-S. Liu, Y. Meng and C.-M. Wang, *Inorg. Chem.*, 2014, **53**, 11498; (*f*) K.-H. Leung, B. He, C. Yang, C.-H. Leung, H.-M. D. Wang and D.-L. Ma, *ACS Applied Materials & Interfaces*, 2015, **7**, 24046.

2 (*a*) D. Xia, B. Wang, B. Chen, S. Wang, B. Zhang and J. Ding, *Angew. Chem., Int. Ed.*, 2014, **53**, 1048; (*b*) T. Giridhar, C. Saravanan, W. Cho, Y. G. Park, J. Y. Lee and S.-H. Jin, *Chem. Commun.*, 2014, **50**, 4000; (*c*) J.-L. Liao, Y. Chi, Z.-T. Sie, C.-H. Ku, C.-H. Chang, M. A. Fox, P. J. Low, M.-R. Tseng and G.-H. Lee, *Inorg. Chem.*, 2015, **54**, 10811; (*d*) P. Tao, W.-L. Li, J. Zhang, S. Guo, Q. Zhao, H. Wang, B. Wei, S.-J. Liu, X.-H. Zhou, Q. Yu, B.-S. Xu and W. Huang, *Adv. Funct. Mater.*, 2016, **26**, 881; (*e*) W. Mroz, R. Ragni, F. Galeotti, E. Mesto, C. Botta, L. D. Cola, G. M. Farinola and U. Giovanella, *J. Mater Chem. C*, 2015, **3**, 7506; (*f*) Y.-L. Deng, L.-S. Cui, Y. Liu, Z.-K. Wang, Z.-Q. Jiang and L.-S. Liao, *J. Mater. Chem. C*, 2016, **4**, 1250; (*g*) K. J. Suhr, L. D. Bastatas, Y. Shen, L. A. Mitchell, B. J. Holliday and J. D. Slinker, *ACS Applied Materials & Interfaces*, 2016, **8**, 8888; (*h*) X. Yang, Z. Feng, J. Zhao, J.-S. Dang, B. Liu, K. Zhang and G. Zhou, *ACS Applied Materials & Interfaces*, 2016, **8**, 33874.

3 (*a*) E. Baggaley, J. A. Weinstein and J. A. G. Williams, *Coord. Chem. Rev.*, 2012, **256**, 1762; (*b*) K. K.-W. Lo and K. Y. Zhang, *RSC Adv.*, 2012, **2**, 12069; (*c*) L. He, C.-P. Tan, R.-R. Ye, Y.-Z. Zhao, Y.-H. Liu, Q. Zhao, L.-N. Ji and Z.-W. Mao, *Angew. Chem., Int. Ed.*, 2014, **53**, 12137; (*d*) A. Kando, Y. Hisamatsu, H. Ohwada, T. Itoh, S. Moromizato, M. Kohno and S. Aoki, *Inorg. Chem.*, 2015, **54**, 5342.

4. H. Sun, S. Liu, W. Lin, K. Y. Zhang, W. Lv, X. Huang, F. Huo, H. Yang, G. Jenkins, Q. Zhao and W. Huang, *Nat. Commun.*, 2014, **5**, 4601.

5 (*a*) J. I. Goldsmith, W. R. Hudson, M. S. Lowry, T. H. Anderson and S. Bernhard, *J. Am. Chem. Soc.*, 2005, **127**, 7502; (*b*) M. S. Lowry, J. I. Goldsmith, J. D. Slinker, R. Rohl, R. A. Pascal, Jr., G. G. Malliaras and S. Bernhard, *Chem. Mater.*, 2005, **17**, 5712; (*c*) Y.-J. Yuan, Z.-T. Yu, H.-L. Gao, Z.-G. Zou, C. Zheng and W. Huang, *Chem. Eur. J.*, 2013, **19**, 6340; (*d*) J.-G. Cai, Z.-T. Yu, Y.-J. Yuan, F. Li and Z.-G. Zou, *ACS Catal.*, 2014, **4**, 1953; (*e*) A. Neubauer, G. Grell, A. Friedrich, S. I. Bokarev, P. Schwarzbach, F. Gartner, A.-E. Surkus, H. Junge, M. Beller, O. Kuhn and S. Lochbrunner, *J. Phys. Chem. Lett.*, 2014, **5**, 1355; (*f*) C. Yang, F. Mehmood, T. L. Lam, S. L.-F. Chan, Y. Wu, C.-S. Yeung, X. Guan, K. Li, C. Y.-S. Chung, C.- Y. Zhou, T. Zou and C.-M. Che, *Chemical Science*, 2016, **7**, 3123 and references therein; (*g*) Y. Kuramochi and O. Ishitani, *Inorg. Chem.*, 2016, **55**, 5702.

6 (*a*) A. M. Bunzli, E. C. Consta ble, C. E. Housecroft, A. Prescimone, J. A. Zampese, G. Longo, L. Gil-Escrig, A. Pertegas, E. Orti and H. J. Bolink, *Chem. Sci.*, 2015, **6**, 2843; (*b*) M. Mauro, K. C. Schuermann, R. Preto, A. Hafner, P. Mercandelli, A. Sironi and L. D. Cola, *Angew. Chem., Int. Ed.*, 2010, **49**, 1222.

7 (*a*) X. Cao, Y. Wu, K. Liu, X. Yu, B. Wu, H. Wu, Z. Gong and T. Yi, *J. Mater. Chem.*, 2012, **22**, 2650; (*b*) K. Chen, J. W. Bats, M. Shmittel, *Inorg. Chem.*, 2013, **52**, 12863.

8 (*a*) Y. H. Lee, J. Park, J. Lee, S. U. Lee and M. H. Lee, *J. Am. Chem. Soc.*, 2015, **137**, 8018; (*b*) Y. Zhou, W. Li, L. Yu, Y. Liu, X.Wang and M. Zhou, *Dalton Trans.*, 2015, **44**, 1858.

9 (*a*) Y. Wang, N. Sun, B. F. E. Curchod, L. Male, D. Ma, J. Fan, Y. Liu, W. Zhu and E. Baranoff, *J. Mater. Chem. C*, 2016, **4**, 3738; (*b*) M. Marin-Suarez, B. F. E. Curchod, I. Tavernelli, U. Rothlisberger, R. Scopelliti, I. Jung, D. D. Censo, M. Gratzel, J. F. Fernandez-Sanchez, A. Fernandez-Gutierrez, M. K. Nazeeruddin and E. Baranoff, *Chem. Mater.*, 2012, **24**, 2330.

10 (*a*) L. Sun, G. Li, X. Chen, Y. Chen, C. Jin, L. Ji and H. Chao, *Sci. Rep.*, 2015, **5**, 14837; (*b*) N. M. Shavaleev, G. Xie, S. Varghese, D. B. Cordes, A. M. Z. Slawin, C. Momblona, E. Orti, H. J. Bolink, I. D. W. Samuel and E. Zysman-Colman, *Inorg. Chem.*, 2015, **54**, 5907; (*c*) E. C. Constable, M. Neuburger, P. Rosel, G. E. Schneider, J. A. Zampese, C. E. Housecroft, F. Monti, N. Armaroli, R. D. Costa and E. Orti, *Inorg. Chem.*, 2013, **52**, 885; (*d*) N. M . Shavaleev, R. Scopelliti, M. Gratzel, M. K. Nazeeruddin, A. Pertegas, C. Rold an-Carmona, D. Tordera and H. J. Bolin, *J. Mater. Chem. C*, 2013, **1**, 2241; (*e*) Q. Zhao, L. Li, F. Li, M. Yu, Z. Liu, T. Yi and C. Huang, *Chem. Commun.*, 2008, 685; (*f*) S. Sharma, H. Kim, Y. H. Lee, T. Kim, Y. Sup Lee and M. H. Lee, *Inorg. Chem.*, 2014, **53**, 8672; (*g*) S. Ladouceur and E. Zysman-Colman, *Eur. J. Inorg. Chem.*, 2013, 2985.

11 A. J. Hallett, B. D. Ward, B. M. Kariuki and S. J. A. Pope, *J. Organometallic Chem.*, 2010, **695**, 2401.

12 L. Murphy, A. Congreve, L.-O. Palsson and J. A. G. Williams, *Chem. Commun.*, 2010, **46**, 8743.

13 (*a*) A. F. Henwood, Y. Hu, M. T. Sajjad, G. K. V. V. Thalluri, S. S. Ghosh, D. B. Cordes, A. M. Z. Slawin, I. D. W. Samuel, N. Robertson and E. Zysman-Colman, *Chem. Eur. J.*, 2015, **21**, 19128; (*b*) D.-K. Cao, J.-S. Hu, M.-Q. Li, D.-P. Gong, X.-X. Li

View Article Online
DOI: 10.1039/C7DT01337J

and M. D. Ward, *Dalton Trans.*, 2015, **44**, 21008; (*c*) S. A. Rommel, D. Sorsche, N. Rockstroh, F. W. Heinemann, J. Kubel, M. Wachtler, B. Dietzek and S. Rau, *Eur. J. Inorg. Chem.*, 2015, 3730. (d) D.-P. Gong, T.-B. Gao, D.-K. Cao and M. D. Ward, *Dalton Trans.*, 2017, **46**, 275.

14 (*a*) J. Zhai, P. Lei, H.-J. Chi and Z.-Z. Hu, *Chin J. of Synthetic Chem.*, 2005, **13**, 282; (*b*) S. Kappaun, S. Eder, S. Sax, K. Mereiter, E. J. W. List and C. Slugovc, *Eur. J. Inorg. Chem.*, 2007, 4207.

15 SAINT, Program for Data Extraction and Reduction, Siemens Analytical X-ray Instruments, Madison, WI, 1994–1996.

16 (*a*) SHELXTL, Reference Manual, version 5.0, Siemens Indus-trial Automation, Analytical Instruments, Madison, WI, 1997; (*b*) G. M. Sheldrick, *Acta Crystallogr., Sect. A: Fundam. Crystallogr.*, 2008, **64**, 112.

17. E. S. Andreiadis, D. Imbert, J. Pecaut, A. Calborean, I. Ciofini, C. Adamo, R. Demadrille and M. Mazzanti, *Inorg. Chem.*, 2011, **50**, 8197.

18 E. Marchi, R. Sinisi, G. Bergamini, M. Tragni, M. Monari, M. Bandini and P. Ceroni, *Chem. –Eur. J.*, 2012, **18**, 8765.

19 S.-Z. Hu, Z.-X. Xie and C.-H. Zhou, *Acta Phys. -Chim. Sin.*, 2010, **26**, 1795.

20 C. Janiak, *J. Chem. Soc., Dalton Trans.*, 2000, 3885.

21 E. Marchi, R. Sinisi, G. Bergamini, M. Tragni, M. Monari, M. Bandini and P. Ceroni, *Chem. Eur. J.*, 2012, **18**, 8765.

22 (*a*) M. Mydlak, C. Bizzarri, D. Hartmann, W. Sarfert, G. Schmid and L. D. Cola, *Adv. Funct. Mater.*, 2010, **20**, 1812; (*b*) Y. You, S. Lee, T. Kim, K. Ohkubo, W.-S. Chae, S. Fukuzumi, G.-J. Jhon, W. Nam and S. J. Lippard, *J. Am. Chem. Soc.*, 2011, **133**, 18328.

23. T. Sajoto, P. I. Djurovich, A. B. Tamayo, J. Oxgaard, W. A. Goddard III and M. E. Thompson, *J. Am. Chem. Soc.*, 2009, **131**, 9813.

24. (*a*) X.-Y. Li, H.-F. Su, R.-Q. Zhou, S. Feng, Y.-Z.Tan, X.-P. Wang, J. Jia, M. Kurmoo, D. Sun and L-S. Zheng, *Chem.-Eur. J.*, 2016, **22**, 3019; (*b*) H.-Y. Zhuo, H.-F. Su, Z.-Z. Cao, W. Liu, S.-A. Wang, L. Feng, G.-L. Zhuang, S.-C. Lin, M. Kurmoo, C.-H. Tung, D. Sun and L.-S. Zheng, *Chem. -Eur. J.*, 2016, **22**, 17619; (*c*) Z. Wang, G.-L. Zhuang, Y.-K. Deng, Z.-Y. Feng, Z.-Z. Cao, M. Kurmoo, C.-H. Tung and D. Sun, *Inorg Chem*., 2016, **55**, 4757; (*d*) X.-Y. Li, Z. Wang, H.-F. Su, S. Feng, M. Kurmoo, C.-H. Tung, D. Sun and L.-S. Zheng, *Inorg Chem*., 2016, **55**, 1096; (*e*) X.-Y. Li, Z. Wang, H.-F. Su, S. Feng, M. Kurmoo, C.-H. Tung, D. Sun and L.-S. Zheng, *Nanoscale*, 2017, **9**, 3601.

25 (*a*) A. Tsuboyama, H. Iwawaki, M. Furugori, T. Mukaide, J. Kamatani, S. Igawa, T. Moriyama, S. Miura, T. Takiguchi, S. Okada, M. Hoshino and K. Ueno, *J. Am. Chem. Soc.*, 2003, **125**, 12971; (*b*) F. Kessler, R. D. Costa, D. D. Censo, R. Scopelliti, E. Orti, H. J. Bolink, S. Meier, W. Sarfert, M. Gratzel, M. K. Nazeeruddin and E. Baranoff, *Dalton Trans.*, 2012, **41**, 180.

View Article Online
DOI: 10.1039/C7DT01337J

TOC

Compound pidpyH and its Ir(III) complexes $[Ir(dfppy)_2(pidpyH)](PF_6)$ **(1·PF$_6$)** and $[Ir(dfppy)_2(pidpy)]$ **(2)** show TFA-induced luminescence switching behaviors. Compared to **2**, compound **1·PF$_6$** is better photosensitizer, which can be used for reducing water to hydrogen under the irradiation with $\lambda \geq 410$ nm light.